Proceedings of the 37th IEEE
Conference on Decision & Control
Tampa, Florida USA • December 1998

A nonlinear modelling approach to the sugar cane crushing process

Turker Ozkocak Minyue Fu Graham C. Goodwin
Dept. of Elec. and Comp. Eng.,
The University of Newcastle, Callaghan 2308, Australia

Abstract

Compaction of sugar cane varies all through the milling train due to the preparation methods and cane variety. Since compaction is the most crucial variable to influence torque loads and therefore sugar extraction, an adequate model for its estimation is needed. In this paper we put forward a nonlinear dynamical model based on a mass balance principle. The model utilizes the fact that the density of cane bagasse changes approximately linearly with the exerted pressure over it in the operation regions significant to torque control. The model is parametric in two variables which need to be tuned according to the properties of the cane. Our model gives promising results on real plant data and is expected to be useful in nonlinear control of sugar mills.

Key words: nonlinear modelling, sugar mills, sugar cane crushing

1 Introduction

The function of a raw sugar factory is to produce crystal sugar from the juice in sugar canes delivered to the factory. On arrival at the plant, the sugar cane is transported on belt conveyors to the shredder where it is prepared for the removal of juice by the extraction station, see Fig. 1. The shredder prepares the cane by smashing it up into small pieces. The extraction process in Australia is mostly done by crushing mills. The prepared cane from the shredder is passed through a series of mills (typically four to six) called the milling train as a whole. The mills squeeze or crush the cane to separate the juice which contains the sugar from its fibrous part. The fibrous material left after the juice is removed is called bagasse. To help the extraction of juice, some of the produced juice is returned to the bagasse between the mills. Water is also added before the last mill to wash out any remaining sugar. Measurements of bagasse mass and fedback juice flow between mills are often not available, making it difficult to estimate the mass balance. The first milling

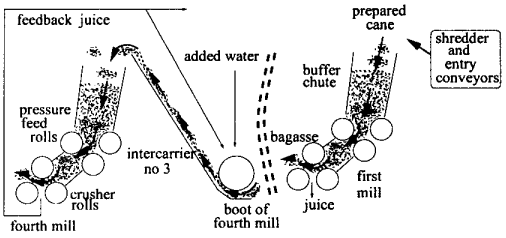

Figure 1: The milling train and related sensors

unit is the major factor in the overall efficiency of the train. This mill is controlled to maintain the throughput rate set by the speed of upstream belt conveyors. All the other mills are controlled to achieve high overall extraction. What differs them from the first mill is that they process bagasse delivered by a fixed speed inter-carrier from the previous mill. From the carrier the bagasse is fed into a buffer chute where the volume and exit geometry are changed via a flap. The free falling bagasse or prepared cane for the first mill are gripped by pressure feed rolls and through another short chute, pushed into crusher rolls. At the exit of crusher rolls the bagasse dives into a boot where it absorbs fedback juice or water. From the boot the bagasse is carried away via a fixed speed carrier into the buffer chute of the preceding mill. The pressure feed and crusher rolls are driven by steam turbines. Gear boxes are coupled between the turbine and the rolls. There is one steam turbine per mill.

The primary objective of mill control is to maximize the extraction at a determined production rate. On average 2.4% of sugar is not extracted. For a plant with a production

0-7803-4394-8/98 $10.00 © 1998 IEEE

capacity of 550 tons/hr, the loss per hour is worth 700 AUD. The gross annual throughput of Australia is 5 million tons. Accordingly the gross annual extraction loss of Australian Sugar Industry is around 40 million AUD.

To achieve a high extraction, it is required to have a high average roll torque. Also smooth control must be maintained around the set point so that possible deviations at the torque due to sudden changes in the cane variety will not damage the machinery. In the current practice, torque control is achieved by changing the chute geometry via the flap while height control is maintained by changing the turbine speed. The height of the material in the buffer chute must be at a level to enable an adequate degree of compaction of the material for efficient crushing . However, it is well-known that the chute height and torque are closely coupled. The aforementioned "decoupled" control scheme is non-ideal.

2 Previous Efforts

The crushing process has been subject to a number of studies in the past. Works by Murry and Holt [5] and Loughran [3] are aimed at a better understanding of the process to improve the mill settings and cane preparation methods. The resultant models are nonlinear, static, and based on parameters which are difficult to estimate in practice.

The work carried out by Partanen [4] involves iterative closed-loop black-box identification in conjuction with LQG based controller design. Although more successful than the current practice the technique suffers from a significant degree of complexity which makes it difficult to maintain efficiently in the lack of a highly skilled control expert.

For control purposes, a simple model which can capture the gross dynamic behaviour is needed. This idea was the motivation for a masters' thesis submitted by Mark West in our department in 1997, [2]. Well-known physical behaviours coupled with information gathered from step tests were combined for modeling. The resultant model is a linear two-input, two-output system that links the manipulating variables, flap position and mill speed, to the controlled variables, torque and chute height. Although quite helpful for qualitative analysis, the lack of inclusion of the material property, which is the major disturbance, prevents the model from capturing the whole spectrum of operation.

The nature of the model that we seek has already been defined: It needs to be simple enough for online purposes but complex enough to capture the key properties of the cane for extraction purposes.

3 A nonlinear compaction model : α-β model

Each mill consists of a buffer chute, a flap, pressure feed rolls, a pressure feed chute, crusher rolls and a boot that is the entry of the inter-carrier which feeds the preceding mill. A diagram is given in Fig. 2

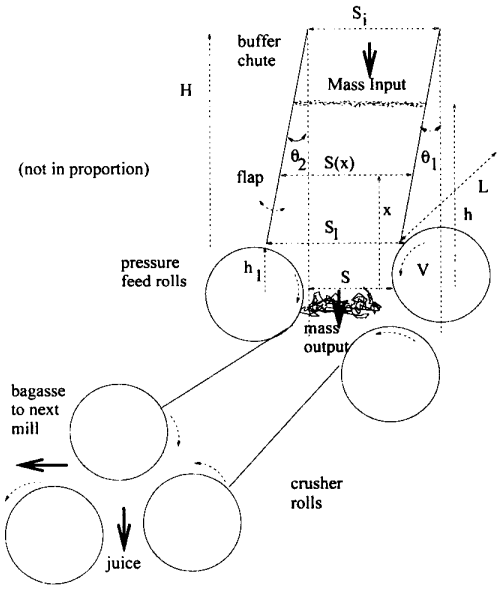

Figure 2: Diagram of Each Mill

where

H	:	Height of the chute
h	:	Height of the material in the chute
$h1$	:	Radius of the top two rolls
S_i	:	Length at the top
S_1	:	Length at height h_1
S	:	Roll gap between the top two rolls
L	:	Width of the system
V	:	Surface speed of rolls
θ_1	:	Vertical angle of the fixed surface
θ_2	:	Vertical angle of the flap

The static pressure-compression characteristics of prepared canes and bagasses are well

known. The results of the experiments done by Noel Deerr [1] are summarized in Fig 3. The pressure drop across the chute is often less than 1 atm. According to the figure, in the low pressure region, the relation between pressure and compression is approximately affine. From the above observation, we propose the

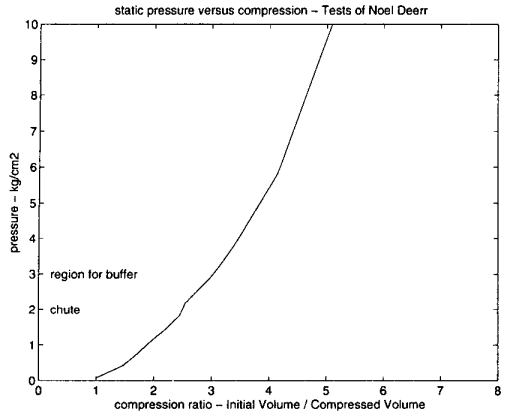

Figure 3: Operation region at low pressure

following relationship for pressure versus density along the chute height.

$$d(x) = \alpha P(x) + \beta \tag{1}$$

The static pressure at any height through the chute is the sum of the weight of the material and atmospheric force acting on its cross section. Denoting by $A(x)$ the cross-sectional area of the chute at height x, we have

$$P(x)A(x) = \int_x^h A(v)d(v)dv + P_a A(h) \tag{2}$$

where h is the height of the material in the chute and $P_a = 10^4 kgf/m^2$ is the atmospheric pressure. Solving this with respect to pressure, we get :

$$P(x) = \frac{e^{-\alpha x} r(x, \alpha, \beta, h, \theta_2)}{A(x)} \tag{3}$$

where $r(x, \alpha, \beta, h, \theta_2)$ is to be explained later. It follows that the density at any height x is given by:

$$d(x) = \alpha \frac{e^{-\alpha x} r(x)}{S(x)L} + \beta \tag{4}$$

Subsequently, the density of material at the exit of the chute is:

$$d(h_1) = \alpha \frac{e^{-\alpha h_1} r(h_1)}{S_1 L} + \beta \tag{5}$$

The cross sectional area $A(x)$ is

$$A(x) = S(x)L \tag{6}$$

where $S(x)$ is the width of the cross section at x which depends on the flap angle :

$$S(x) = S_1 + (S_i - S_1)\frac{(x - h_1)}{H} \tag{7}$$

and

$$S_1 = S_i + H(\tan(\theta_2) - \tan(\theta_1)) \tag{8}$$

Then, the expression for $r(x)$ reads:

$$\begin{aligned} r(x, \alpha, \beta, h, \theta_2) &= \\ e^{\alpha h}\left(\frac{L\beta}{\alpha}(S_1 - \frac{h_1(S_i - S_1)}{H}) + \right. & \\ \left. \frac{L\beta}{\alpha^2 H}(S_i - S_1)(\alpha h - 1) + 10^4 S(h)L\right) - & \\ e^{\alpha x}\left(\frac{L\beta}{\alpha}(S_1 - \frac{h_1(S_i - S_1)}{H}) + \right. & \\ \left. \frac{L\beta}{\alpha^2 H}(S_i - S_1)(\alpha x - 1)\right), h_1 \leq x \leq h & \end{aligned} \tag{9}$$

Next, we derive a dynamic model for the chute height. To this end, we first note that the output mass flow is approximately given by:

$$M_o = S_1 L V d(h_1) \tag{10}$$

Denoting by $M(t)$ the total mass in the chute at time t

$$M(t) = \int_{h_1}^h d(x)A(x)dx \tag{11}$$

the mass balance for the buffer chute may be written as:

$$M_i - M_o = \frac{dM}{dt} = \frac{\partial M}{\partial h}\frac{dh}{dt} + \frac{\partial M}{\partial \theta_2}\frac{d\theta_2}{dt} \tag{12}$$

The partial derivative of chute mass with respect to height is:

$$\begin{aligned} \frac{\partial M}{\partial h} = L\left(e^{-\alpha h}(S(h)(10^4\alpha + \beta) + \right. & \\ \left. 10^4\frac{(S_i - S_1)}{H}) - 10^4\frac{(S_i - S_1)}{H}\right. & \end{aligned} \tag{13}$$

and the partial derivative of chute mass with respect to θ_2:

$$\begin{aligned} \frac{\partial M}{\partial \theta_2} = (\frac{H}{cos(\theta_2)^2})\left((e^{\alpha h} - 1)(\frac{\beta L}{\alpha}(1 - \right. & \\ \frac{(h - h_1)}{H} + \frac{1}{\alpha H}) + (1 - \frac{(h - h_1)}{H}L10^4)) - & \\ e^{\alpha h_1}\frac{\beta L}{\alpha^2}(\frac{1}{h_1} + \frac{1}{H}) + \frac{\beta L}{\alpha}(1 - \frac{(h - h_1)}{H} + & \\ \left. \frac{1}{\alpha}(\frac{1}{h_1} + \frac{1}{H}))) + \frac{\beta L}{\alpha}(1 + \frac{(h_1 - h)}{H})\right) & \end{aligned} \tag{14}$$

By now, our nonlinear compaction model is completely described. Since our model involves two major parameters α and β, we will refer to it as the α-β model. These parameters depend on the cane properties and must be estimated for each variety. To verify our model, Eqn. (12) is solved with respect to height and a comparison between the calculated and actual heights is taken to be a measure for the verification of our model.

4 Experiments

The mill considered for the tests is at the CSR Macknade Mill on the Herbert River north of Townsville, Queensland, Australia. The mill is a sensor weak case from the multivariable control point of view. The only continuous weight measurement is done on conveyor belts via a belt weigher before the chute entry of the first mill. The mass flow measurements of extracted juice at mill no 1 and the added water before the entry of mill no 4 are continuous. For every mill actual values for flap position, roll speeds and chute height are available. Every mill is driven by a dedicated steam turbine. The total torque generated at each of those turbines is calculated based on turbine chest, exhaust pressures and speeds. For mill 1 and mill 4 the torque measurements for pressure feeder and crusher roll groups are available. The loads on the electrical drives of all three intermediate carriers are also available as current measurements. Data was logged during both open and closed loop operation.

Open loop tests for a particular mill were done while the height and speed were controlled manually by the operator. In that mode, speed and flap position were changed in steps around the operating point. Due to the couplings and persistent disturbances it was very difficult to apply steps for long. As being the most critical stand, mill 1 could not be held in open loop more than 12 minutes, much shorter than for downstream mills. Due to the slow nature of the process a sampling period of 0.5 sec was chosen.

Since the critical mills, no 1 and no 4, were equipped with more adequate sensors including separate torque measurements for crusher and feeder roll assemblies, we decided to start our analysis with them.

Our model must be able to estimate density variations in the chute well enough to be extended further into the analysis of torque and extraction where material compaction is shown to be important. A correct expression of mass balance is essential. The closeness between the calculated and actual heights is the main evidence of a good model. Accordingly Eqn. (12) was implemented in MATLAB for selected data groups from mill 1 and 4. α and β values which would give the least square error between the real and calculated heights were searched over a space. The search space was limited by an upper bound on the possible material density. It is known that prepared cane has density values around 300-400 kg/m^3 whereas the no-void density of the material is approximately 1130 kg/m^3. Fibre density may be taken as constant at 1530 kg/m^3. So search space for α was defined to be [0.0001-0.2] where β changed over the region [0-500]. Finding α and β values which would estimate the height with a reasonable LSE was thought to be the measure of how good the α-β model explains the process in terms of material characteristics. It must be noted that α and β values depend on the cane variety and preparation methods which are subject to change all through the operation.

Experimental Results for Mill No 1
For mill no 1, the parameter search was done over three data sets:

1. Group M1-STA includes 800 seconds of mill no 1 measurements where a total startup and stop sequence in closed loop is captured.

2. Group M1-G1 includes 200 seconds of mill no 1 measurements in manual operation.

3. Group M1-OL includes 1250 seconds of mill no 1 measurements mainly in automatic mode everywhere but the region covered by M1-G1.

The results are summarized in Figures 4, 5, 6. The parameters found are reasonably close to each other. The density of the prepared cane is estimated to be changing around 450 kg/m^3 which is reasonable in practice. The model is shown to be adequate enough to predict the density variations provided that the correct mass input flow rate is used.

Experimental Results for Mill No 4
For mill no 4, the parameter search was done over three data sets where all three were logged in manual mode.

1. Group M4-G1 includes 2000 seconds of mill no 4 measurements.
2. Group M4-G2 includes 250 seconds of mill no 4 measurements.
3. Group M4-G3 includes 1000 seconds of mill no 4 measurements.

The major problem for mill no 4 was the lack of measurement of input mass flow. The only continuous mass flow rate is measured 30 secs before the chute entry of mill 1. However loads on the electrical drives of the inter-carriers were available as current measurements. The inter-carrier feeding mill no 4 causes a transport lag of 40 secs. If the total mass over the conveyor at any time is M_c, the power need to pull this mass at constant speed, v, is:

$$\begin{aligned} Power &= M_c \times g \times (\sin(\gamma) + \mu\cos(\gamma)) \times v \\ &= k \times I_L \end{aligned} \quad (15)$$

where g is acceleration due to gravity, γ is the inclination of the conveyor, μ is the friction coefficient, k is a constant and I_L is the measured current. Accordingly at any time the total mass on the carrier must be proportionally related to current load. The delay introduced by the carrier is 40 secs. The average mass input flow rate was thought to be $M_c/40$. So M_i for mill no 4 is written as:

$$M_i = k_{IC3} \times I_L \quad (16)$$

where I_L is the net current after subtracting the load current at idle run. The best result was obtained when 40 secs delay was introduced from the load to the mass input.For our purposes proof of the existence of α-β values for any k_{IC3} values would be enough. Accordingly k_{IC3} is chosen to be 70. All three groups minimized the LSE at very similar α-β values. Results are summarized in Figures 7, 8, 9.

Since M4 G1 and M4 G2 were logged within an hour, their α parameters were much closer compared to M4 G3 which belonged to a batch of another day. The search results demonstrate the adequacy of our model in estimating the mass balance, hence the compaction of the material provided a correct k_{IC3} is used. At correct k_{IC3} the input density of the material, $\alpha\ 10^4 + \beta$, must also be the actual value. For wrong k_{IC3} the same rational relation in input densities is preserved as in gains. This was verified by search for optimum parameters at different gains:

k_{IC3}	20	40	70	110
$G1_\alpha$	0.05	0.095	0.155	0.21
$G1_\beta$	10	0	20	230
$G2_\alpha$	0.049	0.095	0.1515	0.197
$G2_\beta$	0	20	0	300
$G3_\alpha$	0.045	0.095	0.165	0.22
$G3_\beta$	100	70	0	230

The inter-carrier load measurements proved to be efficient in estimating the mass inputs.

5 Conclusions

It is shown that our nonlinear model for sugar mill can adequately estimate the compaction of sugar cane in the buffer chute . With an online estimation scheme, it can be used for height control. Extension of it towards the behaviour of the material inside the rolls may be interesting for better torque control and extraction optimization especially for sensor weak plants.

References

[1] Hugot, E. (1972), "Handbook of cane sugar engineering," Elsevier Publishing Company,new York, pp. 144-149.

[2] West, M. (1997), "Modelling and control of a sugar cane crushing mill", MEECE Thesis, Electrical and Computer Engineering, The University of Newcastle, New South Wales, Australia.

[3] Loughran, J.G. (1990), "Mathematical and experimental modelling of the crushing of prepared sugar cane," PhD thesis, Mechanical Engineering, University of Queensland, Queensland, Australia.

[4] Partanen, A. G. (1995), "Controller refinement with application to a sugar cane crushing mill," PhD thesis, Systems Engineering, Research School of Information Sciences and Engineering, The Australian National University.

[5] Murry, C. and Holt, J. (1967) "The Mechanics of crushing sugar cane," Elsevier Publishing Company, New York .

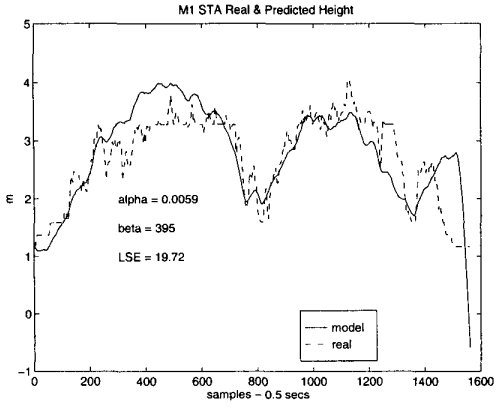

Figure 4: Model performance at best parameters for Mill No 1, group M1-STA

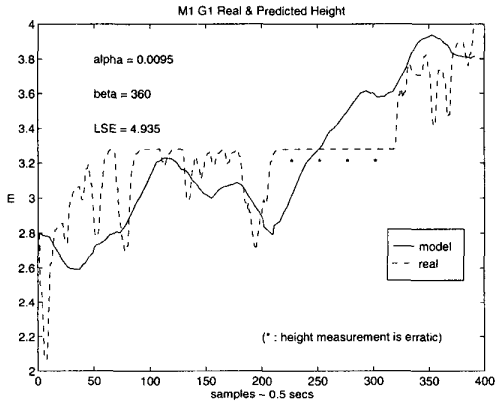

Figure 5: Model performance at best parameters for Mill No 1, group M1-G1

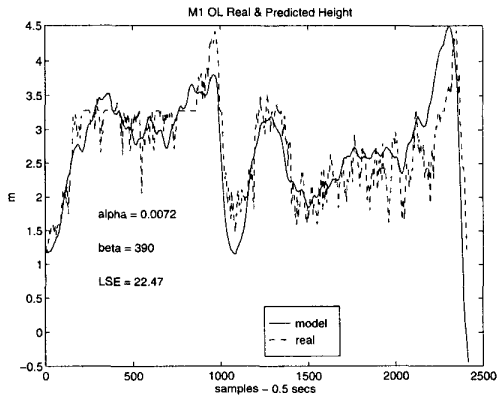

Figure 6: Model performance at best parameters for Mill No 1, group M1-OL

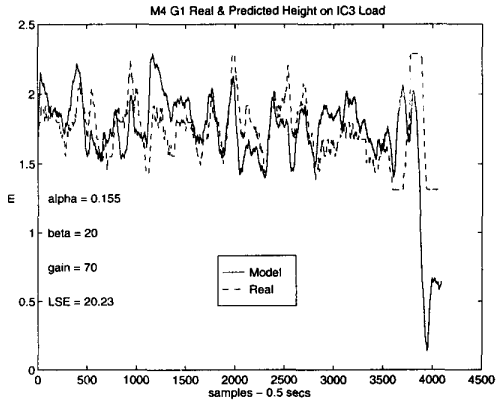

Figure 7: Model performance at best parameters for Mill No 4, group M4-G1

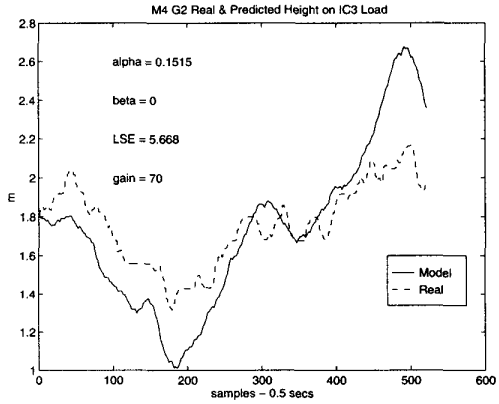

Figure 8: Model performance at best parameters for Mill No 4, group M4-G2

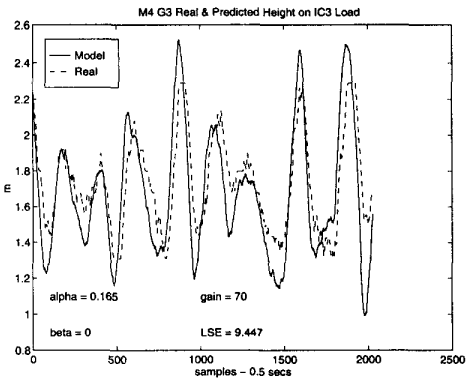

Figure 9: Model performance at best parameters for Mill No 4, group M4-G3